

Scientific Paper

Doi: <http://dx.doi.org/10.1590/1809-4430-Eng.Agric.v42n2e20210043/2022>

SURFACE MOISTURE INDEX BY RADIOMETRIC MEASUREMENTS AND ORBITAL DATA

**Lucimara W. Schirmbeck^{1*}, Denise C. Fontana¹, Juliano Schirmbeck²,
Genei A. Dalmago³, José M. C. Fernandes³**

^{1*}Corresponding author. Universidade Federal do Rio Grande do Sul - UFRGS/ Porto Alegre - RS, Brasil.
E-mail: lucimaraws@gmail.com | ORCID ID: <https://orcid.org/0000-0002-4400-3524>

KEYWORDS

TVDI, ground-based
NDVI system,
Glycine max L.,
agriculture.

ABSTRACT

As an indicator of surface moisture, TVDI has great potential for application in agriculture in different types of climates, but the best results have been obtained in arid climates, given the presence of areas with contrasting water conditions. Some studies under subtropical climate conditions have shown good results in the use of TVDI as an indicator of surface moisture but some uncertainties still need to be better understood. This study aimed to evaluate the coherence of temperature-vegetation dryness index (TVDI) values, obtained from sensors installed on the surface, compared to data obtained using orbital images in an agricultural area in southern Brazil under humid subtropical climate conditions. The analyses employed normalized difference vegetation index (NDVI) and surface temperature (T_s) data obtained through sensors installed on the surface, with continuous monitoring, as well as Landsat OLI/TIRS images, covering the period of the soybean cycle. The TVDI values, obtained from NDVI and T_s radiometric sensors installed in the field, indicated consistency of using Landsat-OLI/TIRS orbital images to map the surface moisture condition, representing the spatial and temporal variations of the water condition of soybean cultivations under subtropical climate conditions.

INTRODUCTION

Vegetation plays an essential role in the energy exchange process on the Earth's surface, modulating energy inputs and outputs, whose flows can be quantified through energy balance (Ryu et al., 2019). Changes that may occur in the soil-water-vegetation system cause alterations in this balance and may lead to yield losses in agricultural areas, being important to be quantified (Fontana et al., 2015; Matzenauer et al., 2020).

In this context, the use of remote sensing, through the application of indices to monitor vegetation in agricultural areas, becomes attractive. The normalized difference vegetation index (NDVI), is an index that expresses the quantity and status of green biomass. On the other hand, surface temperature (T_s) can be obtained through the detection of the energy emitted in the thermal

spectrum, assisting in agricultural monitoring, considering its relationship with the water status of vegetation.

The dispersion in the two-dimensional space between T_s and NDVI is usually triangular (Sandholt et al., 2002; Fuzzo & Rocha, 2018; Schirmbeck et al., 2018). The edges of this triangle define two limits (wet and dry), which are used to calculate an index that expresses the moisture on the surface, the temperature-vegetation dryness index (TVDI). Proposed based on empirical parameterization that considers the strong relationship between T_s and NDVI, TVDI is a simple method, with great potential for application, based on information obtained only from satellites. The index was proposed in a study that covered part of the semi-arid region of Senegal, West Africa, using 37 images from NOAA-AVHRR (Sandholt et al., 2002), but later has been applied using different types of images (Chen et al., 2015; Bai et al., 2017; Uniyal et al., 2017; Sayago et

¹ Universidade Federal do Rio Grande do Sul - UFRGS/ Porto Alegre - RS, Brasil.

² Universidade do Vale do Taquari - UNIVATES/ Lajeado - RS, Brasil.

³ Embrapa Trigo/ Passo Fundo - RS, Brasil.

Area Editor: Fabio Henrique Rojo Baio

Received in: 3-20-2021

Accepted in: 3-28-2021

al., 2017; Holzman et al., 2018; Liu & Yue, 2018, Wang et al., 2020).

As an indicator of surface moisture, TVDI has great potential for application in agriculture in different types of climates, but the best results have been obtained in arid climates, given the presence of areas with contrasting water conditions (Holzman et al., 2018). Some studies under subtropical climate conditions have shown good results in the use of TVDI as an indicator of surface moisture (Schirmbeck et al., 2017b 2018), but some uncertainties still need to be better understood.

Sensors installed in towers on a local scale on the surface, continuously monitoring vegetation and collecting surface data, with technology similar to that used in satellites, are sources of reference data for validating orbital data (Baghzouz et al., 2010; Balzarolo et al., 2011). These data can serve to better understand the functioning of the TVDI index and its limitations,

especially under climate conditions other than those in which the index was proposed.

Based on the current need for agricultural modernization, this study aimed to evaluate the coherence of TVDI values, obtained from sensors installed on the surface, which use technology similar to that of satellites, compared to those obtained using orbital images in an agricultural area in southern Brazil under humid subtropical climate conditions.

MATERIAL AND METHODS

Study area

The study area is located in an agricultural region in southern Brazil, in the state of Rio Grande do Sul, in the Pampa biome, where most of the state's grain production is concentrated (FIGURE 1). The experiment was conducted on-farm.

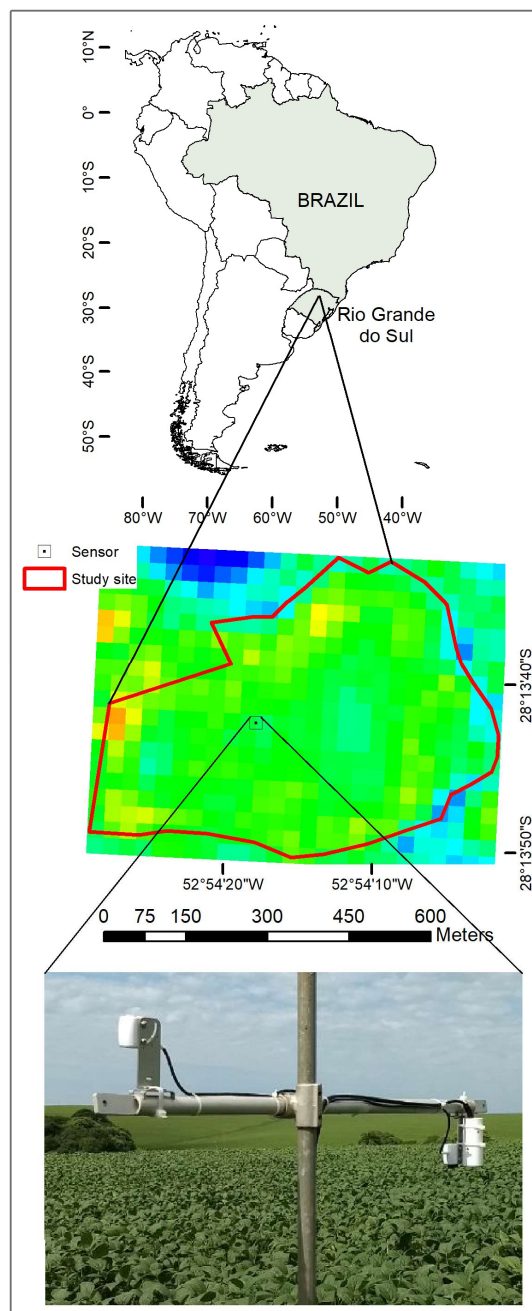


FIGURE 1. Location of the study area in southern Brazil in the state of Rio Grande do Sul. Detail of the sensors installed in the experimental area in the soybean field.

It is a region characterized mainly by agricultural areas of intensive summer and winter uses, with an altimetric variation from 700 to 1,389 m and climate classified as Cfa according to Köppen (Alvares et al., 2013).

The analyses covered the period from spring to summer of 2017-2018. The soybean crop, cultivar DM 5958 RSF IPRO, was sown in November, according to the agricultural calendar (11/13/2017) (Fontana et al., 2015) and the harvest occurred on 04/03/2018.

Surface measurements

Surface measurements included biophysical and radiometric data observed in the vegetation. The leaf area

index (LAI) and phenological stages of soybean are among the biophysical data used to characterize the crop development.

The NDVI and T_s data were also obtained from continuous monitoring, with records every 15 minutes, using the Meter Group - Em50 series data logger. The radiometric sensors were mounted in pairs (T_s /NDVI) on the tower (FIGURE 2), pointing in the same direction, with an angle of 90° at a height of approximately 1 m above the top of the canopy with weekly adjustment. The data from the field sensors were obtained at the time of the satellite passage (10:30 am), with an average of three measurements (10:15, 10:30, and 10:45 am) being extracted.

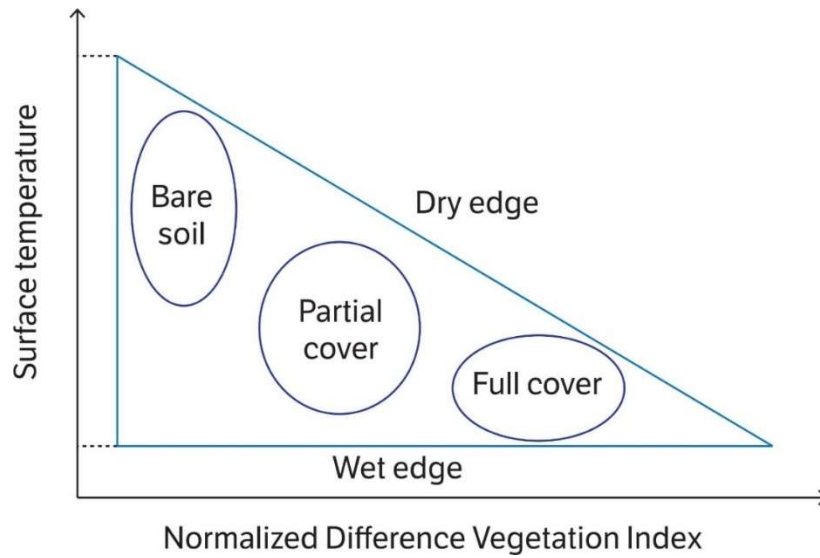


FIGURE 2. Schematic representation of the evaporative triangle in two-dimensional space between the surface temperature (T_s) and the normalized difference vegetation index (NDVI). Source: Schirmbeck et al. (2017a).

The NDVI sensor measured the incident and reflected radiation in the red spectrum (0.6 to 0.7 μm) and near-infrared (0.805 to 0.815 μm) (SRS-NDVI sensor – Meter Group). The hemispherical NDVI sensor was installed facing upwards to measure the incident radiation (FIGURE 2), thus providing the reference values. The other NDVI sensor was installed facing downwards, with the field of view restricted to 20° to measure the reflected radiation from vegetation.

A T_s sensor also facing downwards was coupled next to this sensor to measure the radiation in the thermal spectrum (8 to 14 μm) emitted by the surface (SI 421 sensor - Apogee), with an 18° half-angle field of view.

TVDI

TVDI is obtained from the dispersion between T_s and NDVI (Equation 1), with dispersion in two-dimensional space usually triangular (FIGURE 2) (Sandholt et al., 2002), establishing two limits that serve to normalize the model.

The wet limit is determined by the average T_{smin} , being an indicator of the absence of water deficiency when $TVDI = 0$. The dry limit is an indicator of the existence of water deficiency when $TVDI = 1$. The negative slope of the dry limit line of dispersion is related to the surface evapotranspiration rate, being used to parameterize the model (Chen et al., 2015; Fuzzo & Rocha, 2018). The dry limit is obtained by the linear coefficient a and angular coefficient b of the line obtained from the scatter plot between NDVI and T_s .

$$TVDI = \frac{(T_s - T_{smin})}{(a + b \cdot NDVI - T_{smin})} \quad (1)$$

Where:

T_s is the radiative temperature of the pixel (K);

T_{smin} is the minimum surface temperature (K),

NDVI is the vegetation index, and a and b is the linear and angular coefficients of the line, respectively.

Meteorological water balance and evapotranspiration

The response analysis of the TVDI index relative to the surface water conditions was analyzed through the calculation of the meteorological water balance using the methodology of Thornthwaite & Mather (1955). The meteorological water balance was calculated on a daily scale (Pereira, 2005), considering a K_c between 0.4 and 1.15 (Allen et al., 2006) and a variable available water capacity (AWC) during the cycle depending on the growth of plants and roots throughout the period (Dourado Neto et al. 1999). The reference evapotranspiration was estimated using the Penman-Monteith method (FAO 56) (Allen et al., 2006).

In this analysis, correlations were performed between the main water balance variables that are associated with soil water availability and the TVDI data measured in the field, using a total of 25 days. The T test ($p < 0.05$) was applied using Excel to verify the consistency of the linear correlations.

Landsat OLI/TIRS images

The study area covers 309 pixels of Landsat images, which were used to construct the evaporative triangle. Four images without clouds or noise were obtained during the period of study. The wet and dry limits were defined using an area larger than that studied aiming to contain hot and cold pixels and, therefore, the a , b , and T_{Smin} values, according to the methodology already used (Schirmbeck et al., 2018). The images were taken on November 20 (crop implantation), January 7 and February 8 (vegetative development), and February 24 (beginning of maturation).

TABLE 1. Average values of the normalized difference vegetation index (NDVI), surface temperature (T_s), and temperature-vegetation dryness index (TVDI) obtained from radiometric sensors and Landsat OLI/TIRS images for the entire crop and sampling window on the measurement points (pixel) as a function of the days after sowing (DAS) and phenological stage.

DAS	Image date	Stage	Type	NDVI	LAI	T_s	TVDI
55	Jan./07	R1	Window	0.88		28.31	0.57
			Crop	0.86	5.41	28.69	0.59
			Sensor	0.87		27.98	0.51
			Absolute Error*	0.01		0.33	0.06
87	Feb./08	R5.1	Window	0.93		28.18	0.62
			Crop	0.92	7.76	28.73	0.69
			Sensor	0.9		29.09	0.7
			Absolute Error*	0.03		0.91	0.08
103	Feb./24	R6	Window	0.92		26.76	0.42
			Crop	0.92	6.48	26.98	0.45
			Sensor	0.89		27.21	0.46
			Absolute Error*	0.03		0.45	0.04
Mean Absolut Error*				0.02		0.56	0.06

*error calculated between sensor and window measurement

The lowest NDVI values were observed at 55 days after sowing (DAS) (January 7). On this date, the soybean was at the beginning of flowering (R1 stage), with an LAI = 4.4. Moreover, T_s was high, reaching values close to 28 °C, and TVDI presented intermediate values compared to the other dates.

The two images from February showed NDVI values higher than 0.9, a condition in which the saturation of the index is known to occur (Zhang et al., 2014; Fontana et al., 2015; Mzid et al., 2020) when variations in green biomass do not lead to variations in the index. The period of highest vegetative development occurred in early February, when the crop was at the beginning of grain formation (R1), with an LAI higher than 8, coinciding with the occurrence of high surface temperatures. The high TVDI values expressed the occurrence of water deficiency in the soil-vegetation system in this period of the highest green biomass (TVDI higher than 0.6). In this situation, the leaves close the stomata, thus leading to an increase in the surface temperature (Allen et al., 2006; Chen et al., 2015; Holzman et al., 2018).

Also, the vegetation index is similar for the relationship between the TVDI index and the surface temperature February 8 and February 24 (Schirmbeck et al., 2017b; Uniyal et al., 2017), but the TDVI values reduced on the second date, reflecting the reduction in temperature. Variations in NDVI are slow and continuous throughout the cycle of an annual crop, and thermal variations can reveal

The average values of NDVI, T_s , and TVDI of each image were extracted from a 3×3 window centered on the coordinates in which the sensors were installed. The image data were compared with the sensor measurements.

RESULTS AND DISCUSSION

The results showed consistency between the average data obtained from the crop, the sampling window, and the data measured by the sensors (TABLE 1). The mean absolute errors showed values of 0.02 and 0.56 for NDVI and T_s , respectively, and 0.06 for estimate TVDI.

variations in surface moisture, evidencing the choice of the terms to compose TVDI (Holzman et al., 2018; Schirmbeck et al., 2018).

The precipitation observed at the end of February (70 mm from February 18 to 24) was the only water input in the field and provided better water conditions and, consequently, a reduction in TVDI values. Furthermore, the approach of the autumnal equinox, with reduced energy available on the surface, led to a reduction in solar radiation, decreased the evaporative demand of the atmosphere, and, therefore, the surface temperature (Holzman et al., 2018; Schirmbeck et al., 2018).

FIGURE 3 shows the coherence of the TVDI values measured by radiometric sensors compared with the distribution of the values extracted from images for the 309 pixels that cover the entire crop area. The value measured by the sensors on the two February dates is shown in the central block of the boxplot, which represents 50% of the values observed in the plot. Also, the central block of the boxplot had a small range of values for the three dates, indicating the uniformity of water conditions in the field. Quartiles 0–25% and 75–100% showed higher amplitudes, mainly the upper quartile of the image of February 8. These results may indicate that the calibration of the data set generated by the sensors onboard the Landsat satellite is adequate and generate consistent results when using these data to calculate TVDI (Baghzouz et al., 2010; Balzarolo et al., 2011).

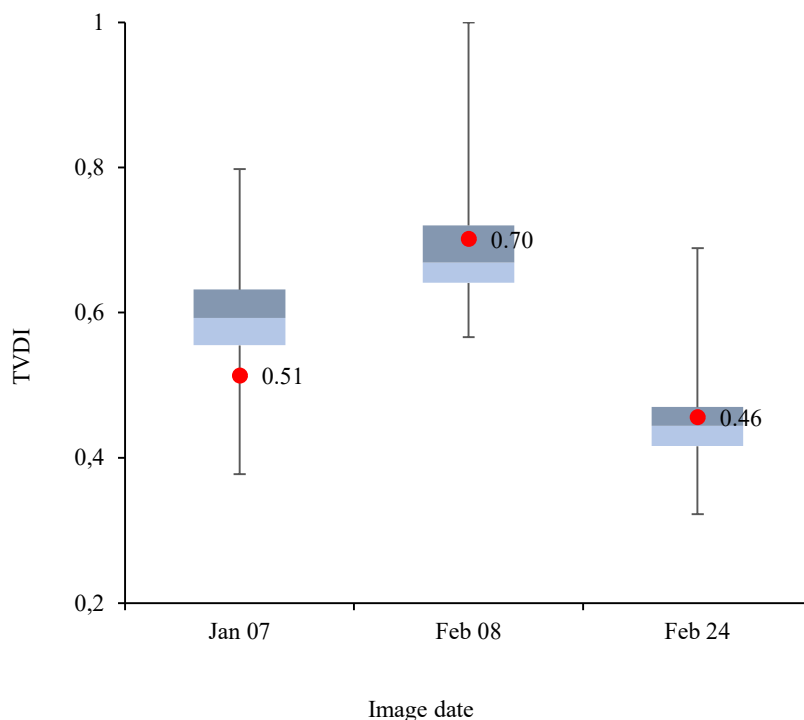


FIGURE 3. Box plot of TVDI data obtained from the pixels that make up the Landsat image. TVDI red dot obtained by field sensor measurements.

The spatial distribution of TVDI in the three dates is shown in FIGURE 4. The range of colors varies from blue to red, and the closer to red, the higher the moisture deficiency on the surface ($\text{TVDI} = 1$). The images evidence the main advantage in using TVDI, that is, the spatialization of information and the possibility of analyzing the index variability in the space of interest. The image of February 8 shows the highest TVDI values in the upper left portion (in red) of the field, pixels that possibly caused the highest

amplitude observed in the boxplot (FIGURE 3). Low variability in water conditions is observed in the cultivation area, which is consistent with the average data (TABLE 1 and FIGURE 3). The images of January 7 and February 8 showed the highest TVDI values, mainly in February. The image of February 24 showed the lowest index values (blue predominates) when the crop was at the grain filling stage, a period that defines the final crop yield (Fontana et al., 2015).

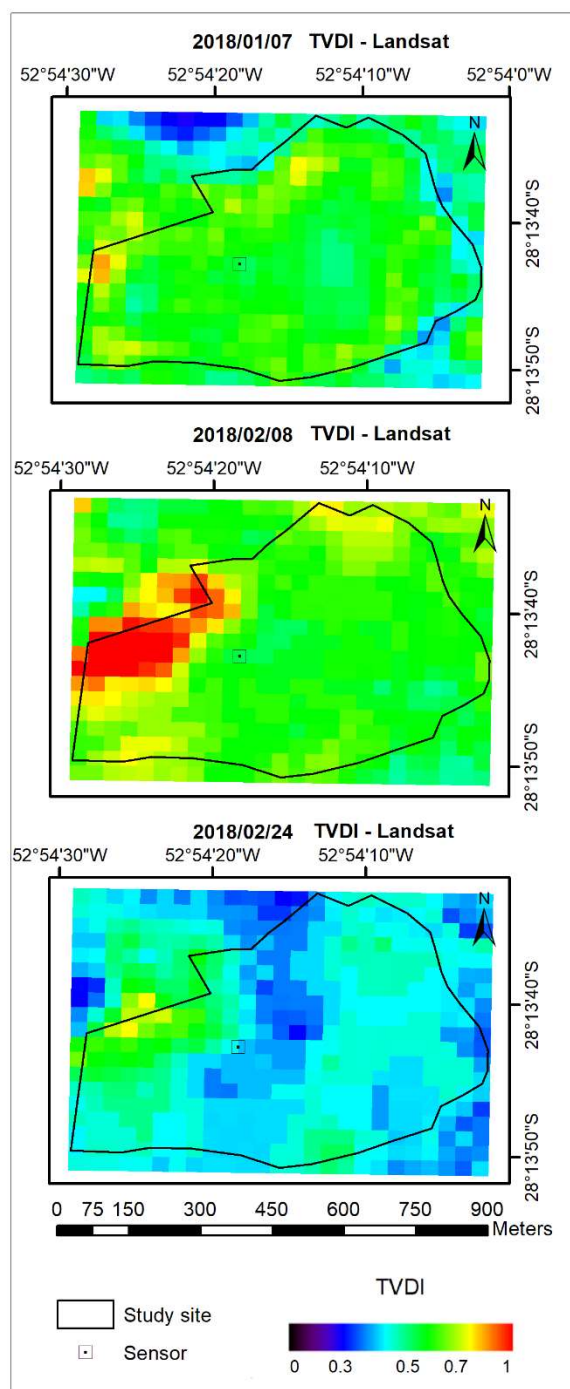


FIGURE 4. Spatial distribution of TVDI for the study area for Landsat OLI/TIRS images of January and February. Detail for the location of the sensor installed on the surface.

The dispersions between TVDI and the main variables obtained from the meteorological water balance, which are associated with water availability, showed an association (FIGURE 5). Positive linear correlations were found between TVDI and water deficit and negative correlations between TVDI and soil water storage, ETr, and the ETr/ET0 ratio, all significant according to the T test ($p < 0.05$). Among the analyzed variables, soil water storage had the highest

correlation coefficient (-0.72), followed by soil water deficit (0.57). Although the nature of these variables derived from water balance (moisture indicators) is different from the quantity expressed in TVDI, the result is encouraging, as it reveals coherence with what was expected. TVDI was obtained using an average of 309 pixels that cover the soybean crop, and the other variables were obtained using data from the weather station that characterizes the region.

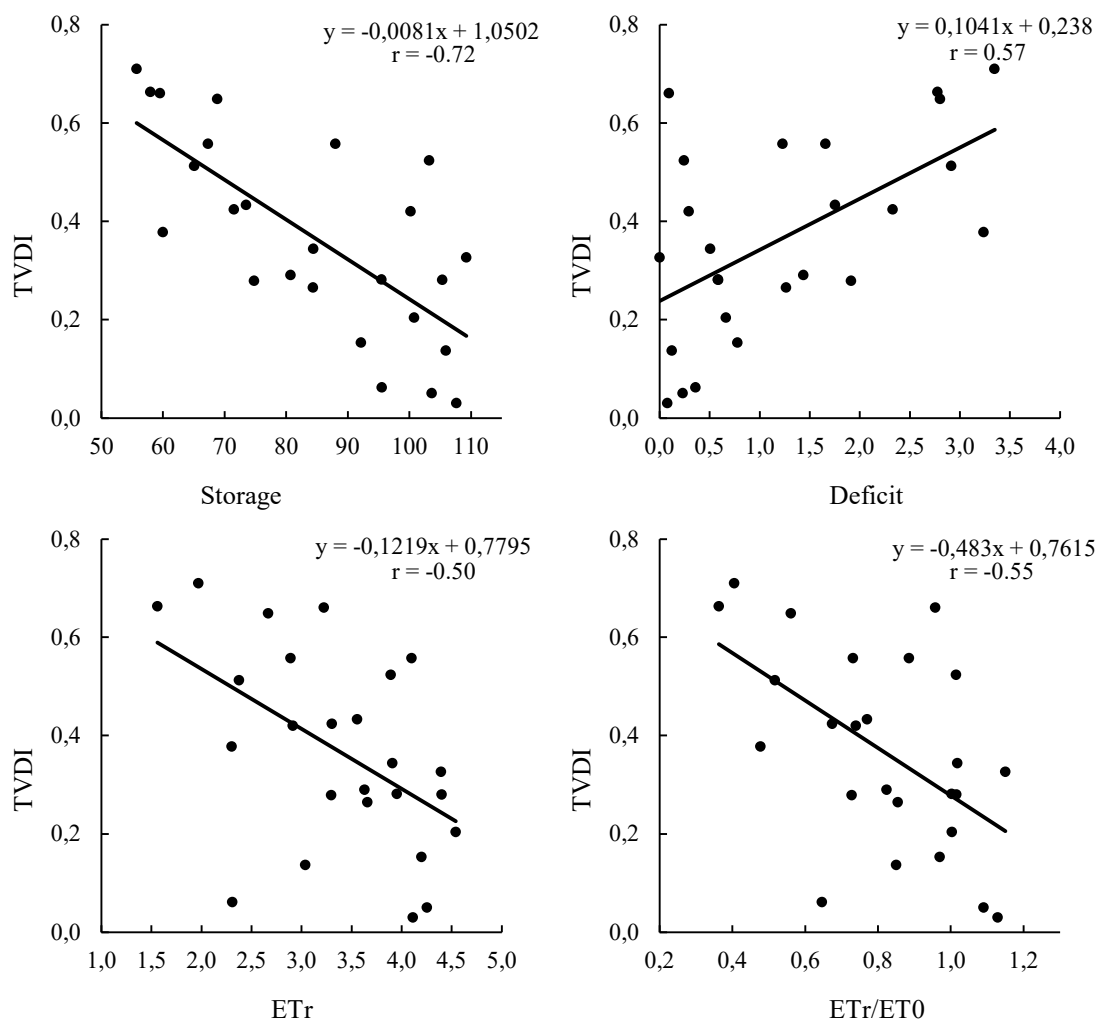


FIGURE 5. Dispersions between TVDI and the main variables derived from the meteorological water balance: Storage, Deficit, ETr, and ETr/ET0.

CONCLUSIONS

These study enable understand the functioning of the TVDI index and showed the coherence of TVDI values, obtained from sensors installed on the surface, which use technology similar to that of satellites.

The similarity of the NDVI and T_s values obtained with surface sensors and those embedded in the Landsat-8 platform also defines similarity in the TVDI values derived from them.

Surface data are obtained with a high degree of measurement control and serve as a reference for the data obtained in the images. The images make it possible to represent the variability of surface moisture conditions within the crop.

TVDI can therefore be recommended as an indicator of surface moisture and assist in agricultural monitoring systems, reducing risks associated with climatic variables and helping decision-making in the sector, becoming important in soybean production areas such as in the southern Brazil.

REFERENCES

- Allen RG, Pereira LS, Raes, D, Smith, M (2006) Evapotranspiración del Cultivo: Guías para la Determinación de los Requerimientos de Agua de los Cultivos. Roma, FAO. 323p. (Irrigation and Drainage Paper, 56).
- Alvares CA, Stape JL, Sentelhas PC, Gonçalves JLM, Sparovek G (2013) Köppen's climate classification map for Brazil. *Meteorologische Zeitschrift* 22:711-728. DOI: <https://doi.org/10.1127/0941-2948/2013/0507>
- Baghzouz M, Devitt D, Fenstermaker LF, Young MH (2010) Monitoring Vegetation Phenological Cycles in Two Different Semi-Arid Environmental Settings Using a Ground-Based NDVI System: A Potential Approach to Improve Satellite Data Interpretation. *Remote Sensing* 2:990-1013. DOI: <https://doi.org/10.3390/rs2040990>
- Bai J, Yu Y, Di L (2017) Comparison between TVDI and CWSI for drought monitoring in the Guanzhong Plain, China. *Journal of Integrative Agriculture*, 16: 389–397. DOI: [https://doi.org/10.1016/S2095-3119\(15\)61302-8](https://doi.org/10.1016/S2095-3119(15)61302-8)

- Balzarolo M, Anderson K, Nichol C, Rossini M, Vescovo L, Arriga N, Calvet JC, Carrara A, Cerasoli Salvatori S, Cogliati S (2011) Ground-based optical measurements at European flux sites: A review of methods, instruments and current controversies. *Sensors* 11:7954-7981. DOI: <https://doi.org/10.3390/s110807954>
- Chen S, Wen Z, Jiang H, Zhao Q, Zhang X, Chen Y (2015) Temperature vegetation dryness index estimation of soil moisture under different tree species. *Sustainability* 7:11401-11417. DOI: <https://doi.org/10.3390/su70911401>
- Dourado Neto D, García AG, Fancelli AL, Frizzzone JA, Reichardt K (1999) Balance hídrico cíclico y secuencial: estimación de almacenamiento de agua em el suelo. *Scientia Agricola* 56(3):537-546. DOI: <https://doi.org/10.1590/S0103-90161999000300005>
- Fontana DC, Pinto, DG, Junges AH, Bremm C (2015) Inferências sobre o calendário agrícola a partir de perfis temporais de NDVI/MODIS. *Bragantia* 74(3):350-358. DOI: <https://doi.org/10.1590/1678-4499.0439>
- Fuzzo DF da S, Rocha JV (2018) Simplify the triangle method for estimating evapotranspiration and its use in agrometeorological modeling. *Pesquisa Aplicada & Agrotecnologia* 11:07-15. DOI: <https://doi.org/10.5935/PAeT.V11.N1.01>
- Holzman ME, Carmona F, Rivas R, Niclòs R (2018) Early assessment of crop yield from remotely sensed water stress and solar radiation data. *ISPRS Journal of Photogrammetry and Remote Sensing* 145:297-308. DOI: <https://doi.org/10.1016/j.isprsjprs.2018.03.014>
- Liu Y, Yue H (2018) The Temperature Vegetation Dryness Index (TVDI) Based on Bi-Parabolic NDVI-Ts Space and Gradient-Based Structural Similarity (GSSIM) for Long-Term Drought Assessment Across Shaanxi Province, China (2000–2016) *Remote Sensing* 10: 959. DOI: <https://doi.org/10.3390/rs10060959>
- Matzenauer R, Maluf JRT, Radin B (2020) Regime de chuvas e produção de grãos no Rio Grande do Sul: impacto das estiagens e relação com o fenômeno El Niño Oscilação Sul. Porto Alegre: Emater/RS-Ascar 133 p. il. color. E-book.
- Mzid N, Cantore V, Mastro G, Albrizio R, Sellami MH, Todorovic M (2020) The Application of Ground-Based and Satellite Remote Sensing for Estimation of Bio-Physiological Parameters of Wheat Grown Under Different Water Regimes. *Water* 12:2095. DOI: <https://doi.org/10.3390/w12082095>
- Pereira AR (2005) Simplicando o balanço hídrico de Thornthwaite-Mather. *Bragantia* 64(2):311-313. DOI: <https://doi.org/10.1590/S0006-87052005000200019>
- Ryu J, Han K, Lee Y, Park N, Hong S, Chung C, Cho J (2019) Different Agricultural Responses to Extreme Drought Events in Neighboring Counties of South and North Korea. *Remote Sensing* 11: 1773. DOI: <https://doi.org/10.3390/rs11151773>
- Sandholt I, Rasmusen K, Andersen J (2002) A simple interpretation of the surface temperature/vegetation index space for assessment of surface moisture status. *Remote Sensing of Environment* 79:213-224. DOI: [https://doi.org/10.1016/S0034-4257\(01\)00274-7](https://doi.org/10.1016/S0034-4257(01)00274-7)
- Sayago S, Ovando G, Bocco M (2017) Landsat images and crop model for evaluating water stress of rainfed soybean. *Remote Sensing of Environment* 198:30-39. DOI: <https://doi.org/10.1016/j.rse.2017.05.008>
- Schirmbeck LW, Fontana DC, Schirmbeck J (2017a) TVDI spatiotemporal pattern of a soybean growing area in humid subtropical climate. *Bragantia* 76:447-455. DOI: <https://doi.org/10.1590/1678-4499.193>
- Schirmbeck LW, Fontana DC, Schirmbeck J (2018) Two approaches to calculate the TVDI in the humid subtropical climate of southern Brazil. *Scientia Agricola* 75:95-172. DOI: <https://doi.org/10.1590/1678-992X-2016-0315>
- Schirmbeck LW, Fontana DC, Schirmbeck J, Mengue VP (2017b) Understanding TVDI as an index that expresses soil moisture. *Journal of Hyperspectral Remote Sensing* 7:82-90. DOI: <https://doi.org/10.29150/jhrs.v7.2.p82-90>
- Thornthwaite CW, Mather JR (1955) The water balance. *Publications in Climatology*. New Jersey, Drexel Institute of Technology. 104p.
- Uniyal B, Dietrich J, Vasilakos C, Tzoraki O (2017) Evaluation of SWAT simulated soil moisture at catchment scale by field measurements and Landsat derived indices. *Agricultural Water Management* 193:55-70. DOI: <https://doi.org/10.1016/j.agwat.2017.08.002>
- Wang H, He N, Zhao R, Ma X (2020) Soil water content monitoring using joint application of PDI and TVDI drought indices. *Remote Sensing Letters* 11:455-464. DOI: <https://doi.org/10.1080/2150704X.2020.1730469>
- Zhang F, Zhang L, Shi J, Huang J (2014) Soil Moisture Monitoring Based on Land Surface Temperature-Vegetation Index Space Derived from MODIS Data. *Pedosphere* 24:450–460. DOI: [https://doi.org/10.1016/S1002-0160\(14\)60031-X](https://doi.org/10.1016/S1002-0160(14)60031-X)